PHILOSOPHICAL TRANSACTIONS OF THE ROYAL SOCIETY A MATHEMATICAL, PHYSICAL & ENGINEERING SCIENCES

Dislocation Slip Systems in Pentaerythritol Tetranitrate (PETN) and Cyclotrimethylene Trinitramine (RDX) [and Discussion]

H. G. Gallagher, P. J. Halfpenny, J. C. Miller, J. N. Sherwood and D. Tabor

Phil. Trans. R. Soc. Lond. A 1992 **339**, 293-303
doi: 10.1098/rsta.1992.0036

Dislocation slip systems in pentaerythritol tetranitrate (PETN) and cyclotrimethylene trinitramine (RDX)

By H. G. Gallagher, P. J. Halfpenny, J. C. Miller and J. N. Sherwood

Department of Pure and Applied Chemistry, University of Strathclyde, Glasgow G1 1XL, U.K.

An examination has been made of the orientation dependence of microhardness determined using a Knoop indenter on the principal habit faces of RDX ({210}) and PETN ({110}). The variations found (RDX, 32–44 kg mm^{-2}; PETN, 13–24 kg mm^{-2}) were consistent with the crystallographic symmetry of the solids and confirm previous estimates obtained using a Vickers indenter. On the basis that the principal deformation mechanism is dislocation slip and that the variation in hardness reflects the orientation of the dominant slip systems to the surface and hence to the faces of the indenter, a theoretical assessment was made using the models of F. W. Daniels and C. G. Dunn and C. A. Brookes, J. B. O'Neill and B. A. W. Redfern of the expected variation in hardness due to this cause. Satisfactory agreement with experiment was obtained using slip systems of the types (010) [001] and {021} [100] for RDX and (110) [1$\bar{1}$1]-type for PETN. This is the first time that this type of analysis has been attempted for such highly anisotropic systems. These assignments were confirmed by etching and by X-ray topographic analysis of the distribution of dislocation alignments around the hardness impressions. The difference in mechanical behaviour of these solids and its possible role in sensitivity to detonation is discussed on the basis of the relative ease of migration of these dislocation systems.

1. Introduction

It is generally accepted that the impact initiation of energetic materials is nucleated by the development of 'hot spots' in the solid matrix. There is much speculation in the literature on the nature and genesis of these regions (Field *et al.* 1992). Some recent theories (Coffey 1981; Armstrong *et al.* 1982) have focused on the potential role of dislocations in this process. These speculations have led in turn to a wider interest in the nature and properties of dislocations in organic solids and in the role of plastic deformation in detonation processes in energetic materials.

Up to the present time the principal evidence for the nature of mechanically induced dislocations has come from etching studies. Examination of the etched {210} surfaces of as grown crystals of RDX led Connick & May (1969) to propose that the principal slip plane was (010). A later examination by Elban *et al.* (1989) failed to confirm this. They obtained evidence for slip on {021} and proposed a potential slip system {021} [100]. In a more detailed study of etched microhardness impressions on

Phil. Trans. R. Soc. Lond. A (1992) **339**, 293–303
Printed in Great Britain

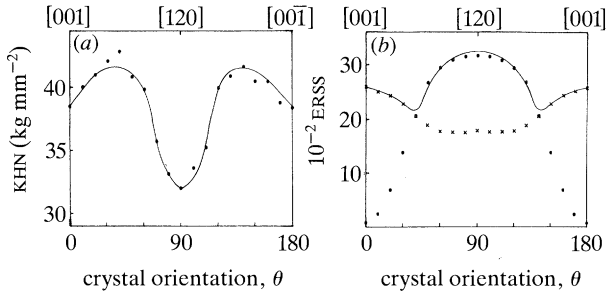

Figure 1. (*a*) The variation of Knoop hardness number (KHN) with crystal orientation (θ) on the {210} habit face of RDX. (*b*) Variation of the orientation dependence of the theoretically derived effective resolved shear stress (ERSS) with crystal orientation for Knoop indentation calculated assuming that the slip systems {021} [100] (×) and (010) [001] (○) are active in the solid. The full line represents the expected variation if both systems are active simultaneously.

all three habit faces Halfpenny *et al.* (1984*a*) confirmed that there were two slip systems. One was defined as (010). Because of the extremely localized nature of the etch pattern around the impression it was not possible to distinguish between {021} and {011} as the second slip plane. Speculatively, on the basis of shortest lattice translations, the primary slip systems were assigned to be {021} or {011} [100] and (010) [001]. More recently Elban *et al.* (1989) have suggested on geometrical grounds that the Burgers vector of the {021} slip system is more likely to be $\pm[01\bar{2}]$.

X-ray topographic examinations of growth defects in RDX have been carried out by McDermott & Phakey (1971*a*, *b*), Lang (unpublished work; see Lang (1978)) and Halfpenny *et al.* (1986). In the last study the Burgers vectors of apparently mobile dislocations were identified as [100] and [001]. The localization of these dislocations in planes (001) and (010) suggests alternative possibilities for slip systems.

For PETN, the situation is less complicated since there is general agreement that the dislocation slip plane is {110}. Speculation varies, however, as to the magnitude and direction of the Burgers vector. Halfpenny *et al.* (1984*a*) favour [001], whereas Dick (1984) proposes the more highly energetic ⟨111⟩. In support of a possible ⟨111⟩ slip direction Halfpenny *et al.* (1984*b*) find this to be the dominant Burgers vector of growth dislocations in crystals prepared by seeded solution growth. It is well known, however, that growth dislocations are not necessarily of similar character to those induced by slip, their formation being defined as much by geometrical conditions at the point of formation as by energetic considerations.

In an effort to resolve these several differences we have carried out a combined theoretical and experimental study of the nature of dislocations induced in these solids by microhardness indentation.

2. Experimental

(*a*) *Crystal growth*

Crystals were prepared by the slow cooling or slow evaporation of saturated solutions of the material in acetone (RDX) and ethyl acetate (PETN) (Hooper *et al.* 1980). The dominant forms (greater than 1 cm^2 area) were RDX: {210} and PETN: {110} and {101}. The specimens selected for study were of low (less than 10^2 cm^{-2}) growth dislocation content, particularly in the external volumes near the bounding facets. The crystal structures of the two materials are:

RDX: orthorhombic, space group $Pbca$, $a = 1.3182$ nm; $b = 1.1574$ nm; $c = 1.0709$ and $z = 8$ (Choi & Prince 1972),

PETN: tetragonal, space group $P\bar{4}2_1c$, $a = b = 0.938$ nm; $c = 0.67$ nm and $z = 2$ (Booth & Llewellyn 1947).

(*b*) *Microhardness indentation*

The orientation dependence of surface hardness of the 'as grown' surfaces was determined using a Leitz miniload microhardness system fitted with a standard Knoop indenter. Indentations were made at 15 g load and at successive 5° intervals rotating the crystal around the normal to the face. Each value of hardness noted below represents the mean of the results from at least 10 indentations made at each orientation. The low load was used to eliminate or minimize cracking around the impression.

(*c*) *Etching*

Crystal surfaces of RDX and PETN were etched following indentation using procedures that have been detailed elsewhere (Connick & May 1969; Halfpenny *et al.* 1984*a*) and which have been proved to be specific for revealing mechanically induced dislocations.

(*d*) *X-ray topography*

Indented crystals were topographed using the Lang transmission technique and CuK_α radiation. Before indentation the crystals were thinned to *ca.* $t = 0.5$ mm thick and the surfaces polished with solvent to remove damage induced by preparation. The geometrical conditions for the topography corresponded to $\mu t \approx 1$ where μ is the absorption coefficient of the radiation.

3. Microhardness indentation

(*a*) *Experimental results*

(i) *RDX*

Hardness impressions were made on the (210) habit surface with 0° corresponding to the indenter long axis lying parallel to [001]. Well defined and regular impressions resulted at all orientations other than 90° ± 5°. Within this range cracks formed along the intersection of the (001) plane with the surface. The experimentally determined variation is shown in figure 1*a*. The Knoop hardness number (KHN) varies considerably with orientation (32–44 kg mm^{-2}) peaking at 40° and 140° from [001] and forming troughs at 90° and 0/180°. No previous Knoop hardness assessments have been made of this solid. The values are consistent, however, with previous studies of Vickers hardness using samples of equivalent quality (VHN 38–39 kg mm^{-2}) (Elban & Armstrong 1981; Halfpenny *et al.* 1984*a*), though higher than the value of 24 kg mm^{-2} quoted by Hagan & Chaudhri (1977).

(ii) *PETN*

The variation in hardness of the (110) face is shown in figure 2*a*. The KHN varies in the range 13–24 kg mm^{-2}. The hardest direction is parallel to [1$\bar{1}$0] and the soft directions lie at ± 15° to [001]. The mirror symmetry around [1$\bar{1}$0] is consistent with the projection of the two dimensional point group symmetry of the material.

Optical examination of the hardness impression showed a high density of slip traces aligned parallel to [001] (figure 4*a*). The extent of the slip lines varied with

PHILOSOPHICAL TRANSACTIONS OF THE ROYAL SOCIETY A MATHEMATICAL, PHYSICAL & ENGINEERING SCIENCES

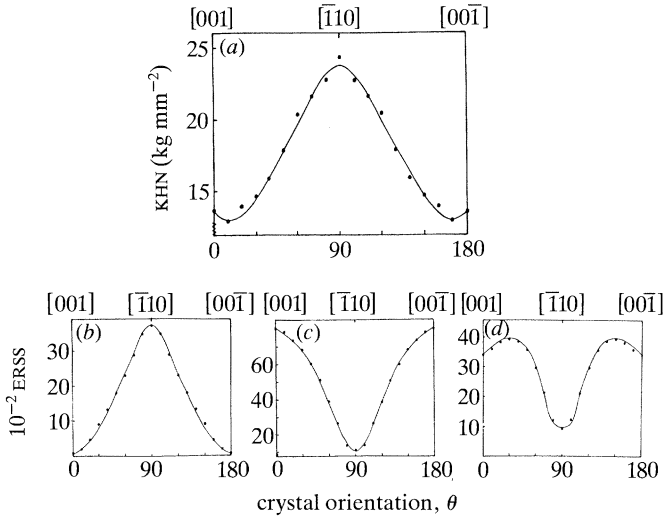

Figure 2. (*a*) The variation of KHN with crystal orientation (θ) on the {110} habit face of PETN. Variation of the theoretically derived ERSS with crystal orientation (θ) for Knoop indentation on the {110} habit face of PETN assuming the dominant slip system (*b*) {110} [001], (*c*) (110) {$\bar{1}$10} and (*d*) (110) [1$\bar{1}$1].

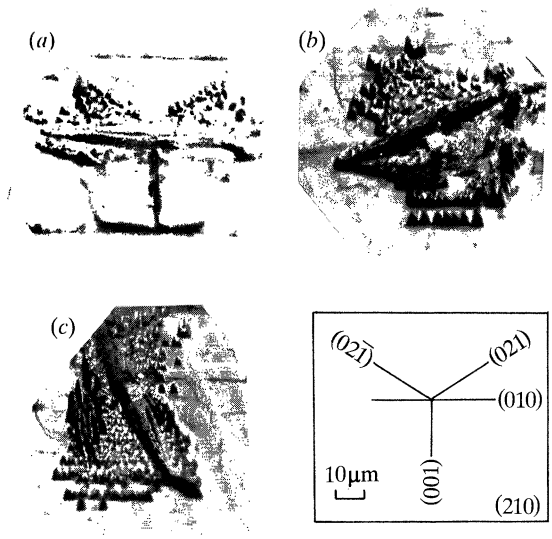

Figure 3. Etch pattern rosettes formed round Knoop indentations on the {210} habit facts of RDX crystals. The separate photo micrograph refers to indentations made with the indenter long axis (*a*) parallel (*b*) at 155° (*c*) at 65° to [001]. The inset (*a*) shows the angles of intersection of the three slip planes (010), (021) and (02$\bar{1}$) with the {210} surface. (Scale mark 10 μm.)

orientation with the maximum extent corresponding to the indenter long axis lying along the hard and soft directions respectively. Some cracking was noted as a consequence of partial cleavage in the (1$\bar{1}$0) planes. This was considerably reduced, however, compared with that previously noted using a Vickers indenter (Hagan & Chaudhri 1977; Halfpenny *et al.* 1984*a*).

(*b*) *Theoretical assessment*

On the basis that the principal deformation mechanism involved in the indentation process is dislocation slip, Daniels & Dunn (1949) have analysed the effective resolved shear stress (ERSS) developed under the Knoop indenter as a function of its orientation to the dominant slip systems. More recently, Brookes *et al.* (1971) have amended and extended the theory to account for some minor discrepancies between theory and experiment in specific systems. Both analyses have been applied successfully to the interpretation of the orientation dependence of the hardness behaviour of a range of solids which are dominantly isotropic in behaviour. We have extended the application of the analysis to the present anisotropic materials as a potential means of distinguishing between the various proposed slip systems.

Using a stereographic projection of the indenter and of the crystallography of the material and its potential slip systems, together with a Wulff net, calculations were made of the variation of the ERSS with surface orientation under the action of several potential slip systems. The result is to yield a mirror image of the theoretical variation of hardness with orientation; the maximum ERSS corresponding always to minimum hardness and vice versa. Absolute values of the hardness cannot be calculated but comparisons of the variations in relative ERSS/hardness are possible. For both materials the analyses of Daniels & Dunn and Brookes *et al.* yielded closely similar variations in phase and differing only in the relative magnitude of the ERSS. We present only those resulting from the analysis of Brookes *et al.*

(i) *RDX*

The results of calculations are presented in figure 1*b* for the potential slip planes (010) and {021} on the assumption that the Burgers vectors of the mobile dislocations correspond to the shortest lattice translations in each case; (010) [001], (021) [100] and (02$\bar{1}$) [100]. A comparison of the combined influence of these slip systems on the total ERSS with the experimentally determined KHN variation shows that each follows a closely similar variation.

Attempts at calculations for other potential slip systems, for example {010} [100] and (021) [01$\bar{2}$] noted as possibilities in the Introduction, yielded variations in ERSS which were completely dissimilar to the observed variation in hardness either separately, or in combination with, other results.

(ii) *PETN*

As noted in the introduction, the slip plane in PETN has been unambiguously defined as {110}. The potential Burgers vectors for dislocation slip on this plane are limited to [001], ⟨110⟩ and ⟨111⟩. The variation of ERSS with orientation for indentation on the (110) face was calculated for the {110} [001], (110) [$\bar{1}$10] and (110) [1$\bar{1}$1]-type slip systems. The curves of ERSS versus orientation for all three systems, based on the latter expression, are shown in figure 2.

The ERSS curve for {110} [001] slip has a maximum along the [$\bar{1}$10] direction and minimum parallel to [001]. This is in direct contradiction to the experimental hardness curve which also has its maximum and minimum along these directions. Therefore, {110} [001] can be discounted as a possible slip system. In contrast, the agreement between the measured hardness and the calculated ERSS for the (110) [$\bar{1}$10] and (110) [1$\bar{1}$1]-type slip systems is much better. In both curves, the position of minimum ERSS lies parallel to the [$\bar{1}$10] direction, corresponding to the hard

direction of surface hardness. Neither plot gives an exact fit to the experimental data in the region around [001]. In each case the maxima in the theoretical curve lie at 15° out of phase with the soft directions indicated by the hardness curve. That for (110) [1$\bar{1}$1] better mirrors the experimental curve since it does predict the observed double minimum in hardness close to [001].

4. Etching studies

(*a*) *RDX*

Confirmation of the proposed slip systems as those dominant in RDX was obtained from etching examination of the hardness impressions. If the theoretical analysis is reliable then the activation of the various slip systems should vary according to the orientation of the crystal surface with respect to the direction of the Knoop indenter. Indentation with the long axis of the indenter parallel to [001] should activate the slip system with the maximum ERSS at this orientation, namely {021} [100]. As the sample is rotated, the ERSS for the {021} slip plane decreases and that for (010) increases until at 35° and 58° from [001] a change-over point occurs where both systems have an equivalent ERSS. From here, slip on (010) becomes increasingly dominant reaching a maximum at 90°. Another changeover point is reached at 130–150°. Finally slip on {021} dominates from 150–180°.

Figure 3*a* shows clearly an etched indentation made with the indenter long axis parallel to [001]. Distinct dislocation etch pit alignments can be seen parallel to the intersection of the (021) and (02$\bar{1}$) planes with the surface. This supports the predicted dominance of these slip systems at this orientation. When an indentation is made at 155° from [001] etching reveals both {021} and (010) alignments (figure 3*b*) although the simultaneous occurrence of slip on both systems spoils the resolution to some extent. As noted above, severe cracking of the surface occurs when indentations are made at 90° to [001]. Alignments of etch pits along the intersection of (010) with the surface are best seen at an indenter orientation of 65° to (010) where, according to the calculations (figure 1*b*), slip on this system should still dominate (figure 3*c*). This combination of excellent agreement of shape and phase of both the experimental hardness and calculated ERSS curves together with the activation of the expected slip traces at the predicted indenter orientation provides confirmation for (010), (021) and (02$\bar{1}$) slip planes and strong evidence for slip systems (010) [001], (021) [100] and (02$\bar{1}$) [100]. These correspond to high energy dislocation types. Their existence is consistent with the low plasticity of the crystal and the limited range of dispersion of dislocation edge pits around the indentation marks (30–50 μm). The results show well the applicability of this type of analysis to anisotropic organic crystals.

(*b*) *PETN*

For PETN, indentation was accompanied by well-defined and relatively extensive slip traces aligned exclusively along the [001] direction corresponding to the intersection of the (1$\bar{1}$0) planes with the surface (figure 4*a*). Variation of indenter orientation produced a greater or lesser extent of slip traces along this direction alone. Etching resulted in the decoration of these slip traces with etch pits (figure 4*b*). Close examination of the etch pit geometry (figure 4*c*) revealed the pits to be hexagonal with mirror symmetry around (1$\bar{1}$0). The apex of the pit is considerably

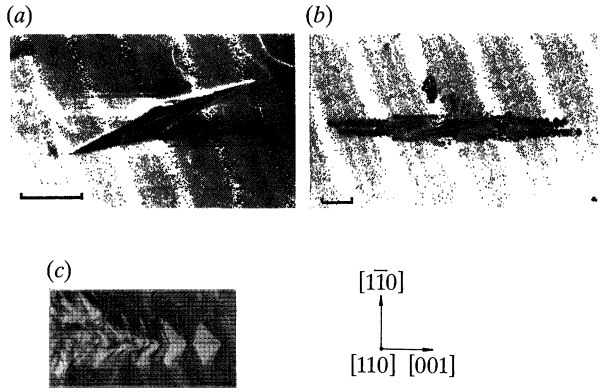

Figure 4. (*a*) Knoop Hardness impression on the {110} habit surface of a PETN crystal showing extensive slip traces. (Scale mark 50 μm). (*b*) At etched Knoop indentation mark on the {110} surface of PETN defining the correspondence of the etch-pit distribution with the slip traces. (Scale mark 50 μm). (*c*) Detail of the shape of the etch-pits in (*b*). (Scale mark 10 μm.)

displaced from the geometrical centre in the (001) direction. Pits on both sides of the indentation were similarly shaped. This asymmetry suggests that the pits are associated with dislocations which lie in the (1$\bar{1}$0) plane at an oblique angle to the (110) face. Of the dislocations considered, only those with a Burgers vector ⟨111⟩ could possibly yield pure edge or screw components for such an inclined dislocation line direction. Etch pits formed at the points of emergence of pure dislocations with Burgers vectors [001] or ⟨110⟩ would be expected to have their apex coincident with the geometric centre of the pit. No etch pits of this type corresponding to mechanical dislocation were ever observed.

We conclude that the etch pits produced around the indentation marks originate at the emergent ends of stress induced dislocation loops which glide on {110} planes with Burgers vector ⟨111⟩. The fact that, on both sides of the indentations, the asymmetric pits are inclined in one direction only implies that only one of the two possible ⟨111⟩ slip directions are active on each of the {110} slip planes.

5. X-ray topography

Confirmatory evidence for the nature of the slip systems in both solids was sought for from contrast variations around X-ray topographic images of the microhardness impressions.

(*a*) *RDX*

For RDX the results were inconclusive. Because of the essentially brittle nature of this solid extensive strain fields are set up in the solid around the point of indentation (see, for example, PETN below). These extend (700 μm) far beyond the limited zone of plastic deformation (*ca.* 30 μm, figure 3) and mask any dislocation images. Attempts to develop more widespread slip by tensile deformation were unsuccessful; fracture occurred before plastic flow again defining the essentially brittle nature of this material.

(*b*) *PETN*

X-ray topography of indentations on the {110} plane of PETN yielded similar but more positive results than for RDX (figure 5*a*).

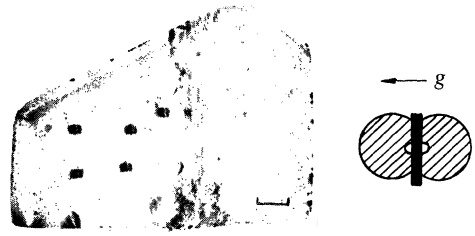

Figure 5. X-ray topograph of indentation marks on the cut and polished (110) face of a PETN crystal ($2\bar{2}0$ reflection). The diagram shows schematically the strain contrast round an indentation. (Scale mark 1 mm.)

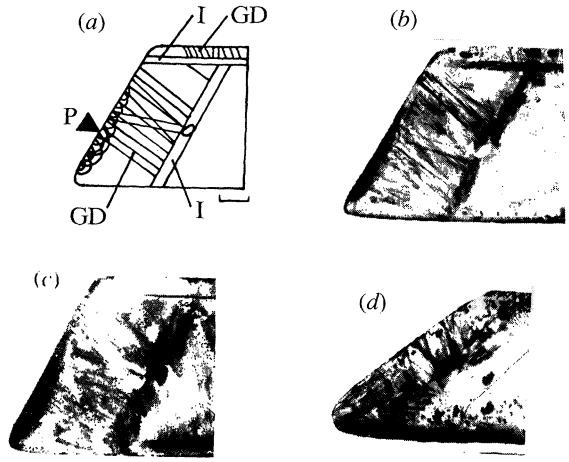

Figure 6. X-ray topographs of a (110) section of a PETN crystal which has been indented on a side ($\bar{1}01$) face. (*a*) Schematic diagram; (*b*) $2\bar{2}0$ reflection; (*c*) 002 reflection; (*d*) $21\bar{1}$ reflection. (P, point of indentation; GD, growth dislocations; I, solvent inclusions.) (Scale mark 1 mm.)

The indentation images show the prominent lobes of dark contrast which correspond to strain induced in the lattice. From an assessment of the extent of the lobes in the various X-ray reflections, it can be concluded that the elastic strain extends, radially, beyond the plastic region for some distance (200 μm) into the lattice. Additionally, a broad line of intensely dark contrast (length 350 μm) parallel to the [001] direction bisects the images. Comparison with the etched indentation mark, shown in figure 4, indicates that the alignment and dimensions of these features corresponds to those of the dislocation slip line traces observed by etching. Therefore, the enhanced contrast can be attributed to dislocations, induced by indentation, which glide on ($1\bar{1}0$) planes. The resolution and hence characterization of individual dislocations is not possible because of the high density of dislocations around the indentation (as indicated by etching) and the relatively low resolution (1 μm) of the X-ray topographic technique.

A number of different X-ray reflections of a second crystal slice indented on the ($1\bar{0}1$) face parallel to (110) are shown in figure 6. Numerous growth dislocations (GD) are observed around the edges of the slice. The majority of these emanate from the two large bands of solvent inclusion (I) and propagate linearly towards the growth faces in both the ($1\bar{1}0$) and ($10\bar{1}$) growth sectors. A lesser number of straight dislocations also emerge into the ($1\bar{1}0$) sector from the interior of the crystal. The

Table 1. *Dislocation slip systems in RDX and PETN*

	slip system	multiplicity	$\boldsymbol{b}$/nm	mobility[a]
RDX	{021} [100]	2	1.32	30–50 μm
	{010} [001]	1	1.07	
PETN	(110) [1$\bar{1}$1]-type	4	1.48	350 μm

[a] Maximum extent of dislocation migration following Knoop indentation at 15 g load.

angle of inclination and the line directions of these dislocations suggest that they originate from the vicinity of the seed. The bands of included solvent probably result from a sudden fluctuation in the temperature during growth. Up to the occurrence of this growth accident, the crystal was relatively free from defects.

In addition to these growth defects, the topographs show considerable darkening around the site of the indentation (P). The enhanced contrast in this region is due to a dense entanglement of stress induced dislocation loops. Close to the (10$\bar{1}$) surface, the dislocations are not completely resolvable, but around the periphery of this strained volume, segments of individual dislocation loops are clearly visible. The geometrical configuration of the loops and their projection in topographs taken using different reflections confirms that they lie on the (110) slip plane.

The Burgers vectors of the dislocation loops were characterized using the invisibility criterion $\boldsymbol{g}\cdot\boldsymbol{b} = 0$, where $\boldsymbol{g}$ = the diffraction vector and $\boldsymbol{b}$ = the Burgers vector (Lang 1978). Recalling that the potential Burgers vector of the glide dislocations are of the [001], ⟨110⟩ and ⟨111⟩ type, we note that the dislocation loops are visible in all but one of the X-ray reflections shown in figure 5. Visibility in the reflections 2$\bar{2}$0 and 002 rules out b [001] and b ⟨110⟩, respectively, as possible Burgers vectors. Despite the residual strain of the growth defects in the 21$\bar{1}$ reflection it is obvious that the strain due to indentation is out of contrast in this reflection. Thus the Burgers vector of the dislocation loops is characterized as [1$\bar{1}$1]. Our tensile tests of suitably oriented specimens have confirmed this result.

6. Discussion

From the above experimental and theoretical analysis the general nature of the principal dislocation slip systems in these materials can be summarized (table 1).

The dislocations identified are all high-energy slip systems which, together with their limited number, low mobility and anisotropy contribute to the essentially brittle nature of these materials under high stress. There are potentially shorter Burgers vectors in the crystal lattice of both materials but these do not appear to be active. Consequently, we must assume that the factors governing the character of mechanically induced dislocations and the active slip systems in organic crystals are rather more complex than in the case of metals and simple ionic compounds. In the latter cases the most favourable slip plane will, in general, be that with the largest interplanar spacing while the shortest lattice translation is the most probable slip direction, since the energy of the dislocation varies as the square of the Burgers vector length. The mechanical properties of organic compounds, however, are influenced by two further factors in addition to these simple packing considerations; first, the nature of the intermolecular bonding and secondly the size and shape of the organic molecule. Although for many organic crystals the cohesive forces are predominantly weak van der Waals interactions, considerable anisotropy of bonding

may occur when hydrogen bonding or permanent dipole–dipole interactions are present. These will exert considerable influence over the nature of the slip systems present. In the case of complex, irregularly shaped organic molecules, certain lattice translations on a given plane will frequently result in energetically unfavourable intermolecular contacts. Such steric effects can dominate the simple geometrical considerations which hold for simple systems (Watanabe & Izumi 1979) leading to the occurrence of long Burgers vectors and slip planes which are not the most closely packed of the structure. It is these steric effects which appear to particularly important in the case of PETN and RDX.

On the basis of simple packing considerations, one would expect the active slip system of PETN to be {110} [001] as these are the most closely packed planes and the shortest lattice translation respectively. Although the slip plane is as predicted, we have shown the slip direction to be $[1\bar{1}1]$, resulting in a considerably longer Burgers vector. In recent work by Dick *et al.* (1991), the intermolecular contacts which occur during the motion of edge dislocations in several possible slip systems are examined. Although these authors do not consider the possible slip system {110} ⟨001⟩, further analysis of these data (J. J. Dick, personal communication) shows that the number of intermolecular contacts in the motion of this system will be two, compared with one for (110) $[1\bar{1}1]$-type. A greater number occur for most other potential slip systems. We are at present attempting similar analyses for RDX.

Dick (1984) has also shown that the number and severity of intermolecular close approaches occurring for various slip systems correlated well with the shock sensitivity of PETN in different orientations. The orientations in which the maximum resolved shear stress slip systems involve low or zero steric hindrance were found to be insensitive while the converse was true for those exhibiting a substantial number of intermolecular close approaches. He suggests that these steric interactions result in direct bond breaking and chemical reactions.

In a similar manner we may speculate upon the relative sensitivities of PETN and RDX in terms of steric effects and active slip systems. It is reasonable to assume that, as has been demonstrated for PETN, the observed active slip systems in RDX do not involve substantial steric hindrance. Therefore, when deformation occurs principally via these systems, the sensitivity of both materials will be low. Our studies have shown that PETN exhibits four possible slip systems, namely (110) $[\bar{1}11]$, (110) $[1\bar{1}1]$, $(\bar{1}10)$ [111] and $(\bar{1}10)$ $[\bar{1}\bar{1}1]$, all of which are symmetrically equivalent. As discussed earlier, the unique asymmetrical etch pit orientations imply that only one Burgers vector per slip plane is active, reducing this number to two. RDX, however, has three active slip systems, (010) [001], $(0\bar{2}1)$ [100] and $(0\bar{2}1)$ [100], the latter two being symmetrically equivalent. So for a random crystal orientation there is a higher probability for RDX that deformation can occur on an active slip system than in the case of PETN. Deformation of RDX is therefore more likely to occur with minimal steric hindrance. We therefore speculate that the substantially higher impact sensitivity of PETN compared with RDX is a direct consequence of fewer available slip systems and a reduced capability for deformation with minimal steric interactions.

The authors gratefully thank the European Office of the US Army (USARDSG-UK) and the US Office of Naval Research, Washington for the financial support of this work.

PHILOSOPHICAL TRANSACTIONS OF THE ROYAL SOCIETY A MATHEMATICAL, PHYSICAL & ENGINEERING SCIENCES

References

Armstrong, R. W., Coffey, C. S. & Elban, W. L. 1982 *Acta metall.* **30**, 2111–2116.

Booth, A. D. & Llewellyn, F. J. 1947 *J. chem. Soc.* 837–846.

Brookes, C. A., O'Neill, J. B. & Redfern, B. A. W. 1971 *Proc. R. Soc. Lond.* A **322**, 73–78.

Coffey, C. S. 1981 *Phys. Rev.* B **24**, 6984–6990.

Choi, C. S. & Prince, E. 1922 *Acta Crystallogr.* B **28**, 2857–2864.

Connick, W. & May, F. G. J. 1969 *J. Crystal Growth* **5**, 65–69.

Dick, J. J. 1984 *Appl. Phys. Lett.* **44**, 859–861.

Dick, J. J., Mulford, R. N., Pettit, D. R., Garcia, E., Spencer, W. J. & Shaw, D. C. 1991 *J. appl. Phys.* **70**, 3572–3587.

Elban, W. L., Armstrong, R. W., Yoo, K. C., Rosemeier, R. G. & Yee, R. Y. 1989 *J. Mater. Sci.* **24**, 1273–1280.

Daniels, F. W. & Dunn, C. G. 1949 *Trans. Am. Soc. Metals* **41**, 419–439.

Field, J. E., Bourne, N. K., Palmer, S. J. P. & Walley, S. M. 1992 *Phil. Trans. R. Soc.* A **339**, 269–283 (this volume).

Hagan, J. T. & Chaudhri, M. M. 1977 *J. Mater. Sci.* **12**, 1055–1058.

Halfpenny, P. J., Roberts, K. J. & Sherwood, J. N. 1984*a* *J. Mater. Sci.* **19**, 1629–1637.

Halfpenny, P. J., Roberts, K. J. & Sherwood, J. N. 1984*b* *J. appl. Crystallogr.* **17**, 320–327.

Halfpenny, P. J., Roberts, K. J. & Sherwood, J. N. 1986 *Phil. Mag.* **53**, 531–542.

Hooper, R. M., McArdle, B. J., Narang, R. S. & Sherwood, J. N. 1980 In *Crystal growth*, 2nd edn (ed. B. Pamplin), pp. 395–420. Oxford: Pergamon.

Lang, A. R. 1978 In *Diffraction and imaging techniques in materials science* (ed. S. Amelinex, R. Gevers & J. Van Landuyt), pp. 623–714. North Holland: Amsterdam.

McDermott, I. T. & Phakey, P. P. 1971*a* *Phys. Stat. Sol.* **8**, 505–571.

McDermott, I. T. & Phakey, P. P. 1971*b* *J. appl. Crystallogr.* **4**, 479–481.

Watanabe, T. & Izumi, K. 1979 *J. Crystal Growth* **46**, 747–756.

Discussion

D. Tabor (*Cambridge University, U.K.*). It is suggested that slip will occur in those directions for which the resolved shear stress is a maximum. Is this an adequate criterion in the hardness test with the Knoop or Vickers indenter? Should account be taken of the fact that the displaced material must be able to flow out of the specimen. Slip in an otherwise favourable direction might be blocked by surrounding material. Nevertheless, there is excellent agreement between the variations of indentation hardness with orientation and the corresponding resolved shear stress assumption; it is very convincing. However, a tensile test, in which there is no blockage of dislocation movement, would give better defined conditions of slip directions.

J. N. Sherwood. This is certainly a problem and ideally allowance would be made for this. It would, however, be a complex problem to solve. We have attempted to minimize this influence by using a low stress. Under these conditions, the hardness impressions are 'sharp' with only minor evidence of material flow out of the indentation. This, plus the good agreement between theory and experiment for the defined slip systems, gives us confidence that slip is the dominant influence. Tensile tests are more reliable for the reason which you note. Using these with PETN we have been successful in confirming the slip system defined from the hardness studies. We have yet to be successful with RDX. With PETN we now hope to move to definitive studies of the behaviour of dislocations in these materials.

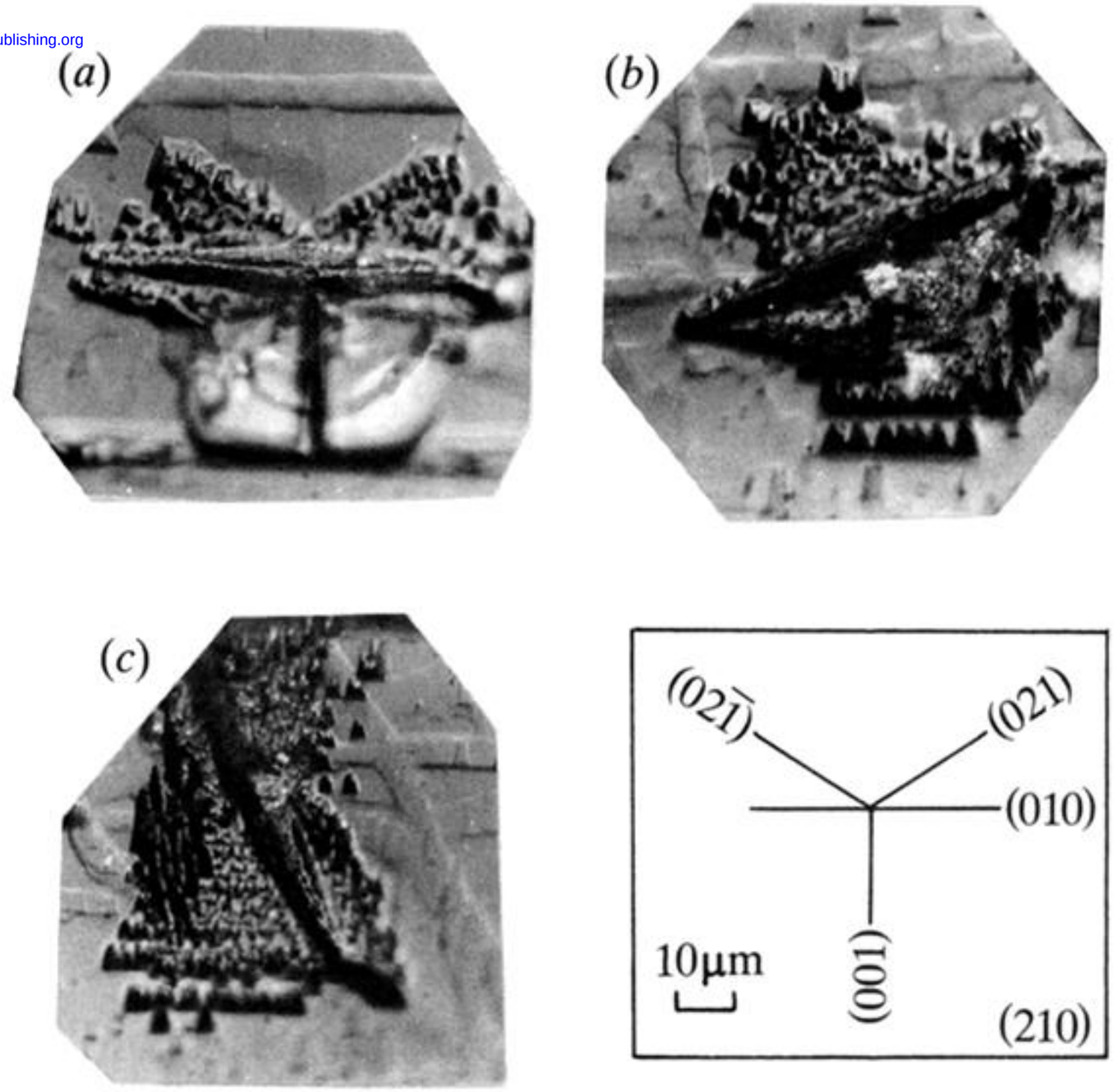

Figure 3. Etch pattern rosettes formed round Knoop indentations on the {210} habit facts of RDX crystals. The separate photo micrograph refers to indentations made with the indenter long axis (*a*) parallel (*b*) at 155° (*c*) at 65° to [001]. The inset (*a*) shows the angles of intersection of the three slip planes (010), (021) and (02$\bar{1}$) with the {210} surface. (Scale mark 10 μm.)

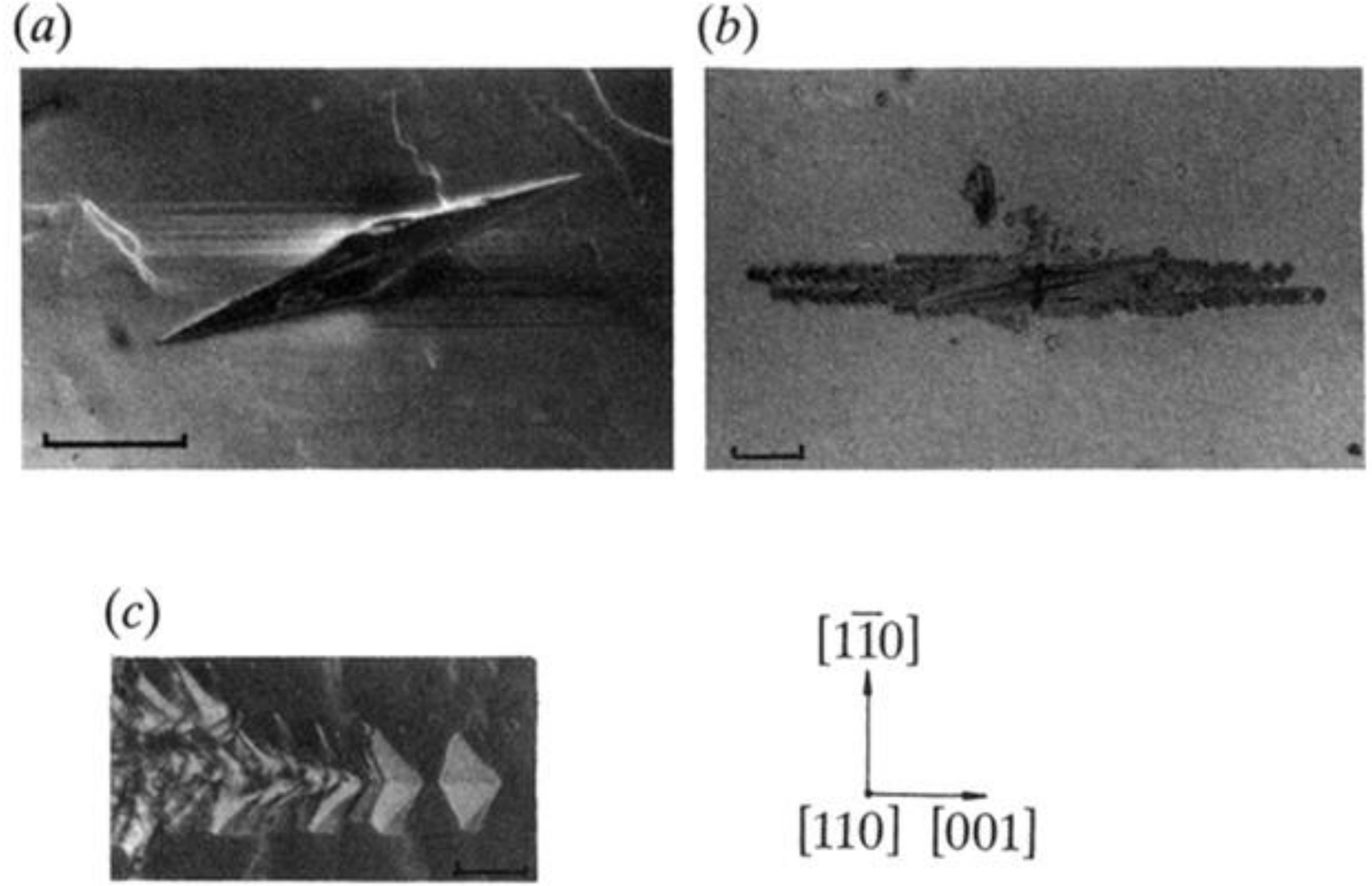

igure 4. (*a*) Knoop Hardness impression on the {110} habit surface of a PETN crystal showing xtensive slip traces. (Scale mark 50 μm). (*b*) At etched Knoop indentation mark on the {110} rface of PETN defining the correspondence of the etch-pit distribution with the slip traces. (Scale ark 50 μm). (*c*) Detail of the shape of the etch-pits in (*b*). (Scale mark 10 μm.)

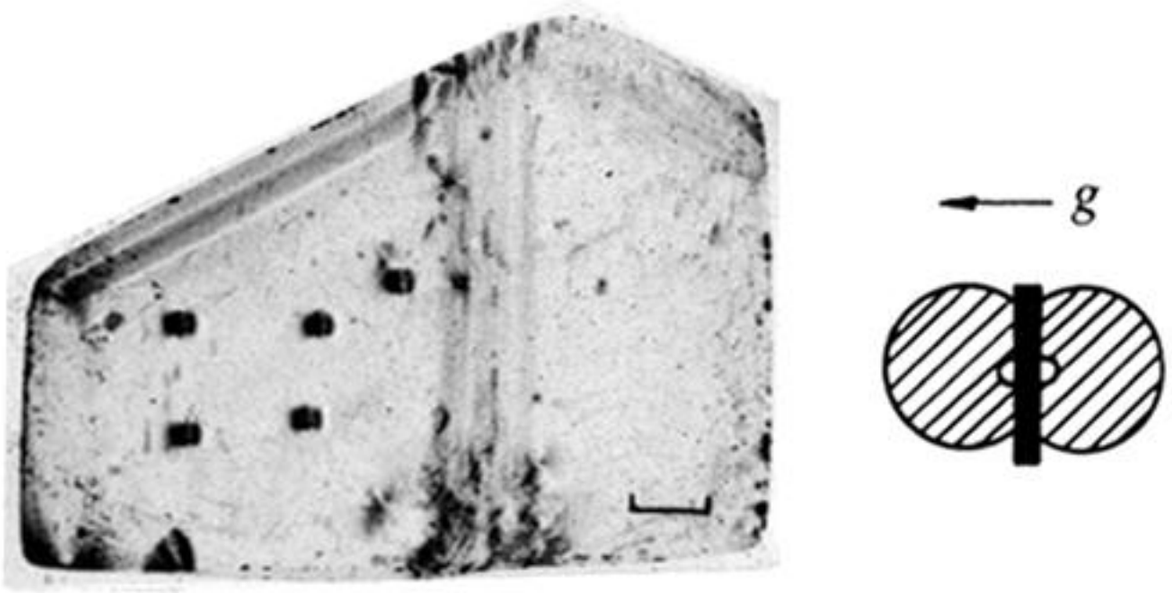

igure 5. X-ray topograph of indentation marks on the cut and polished (110) face of a PETN rystal ($2\bar{2}0$ reflection). The diagram shows schematically the strain contrast round an indentation. Scale mark 1 mm.)

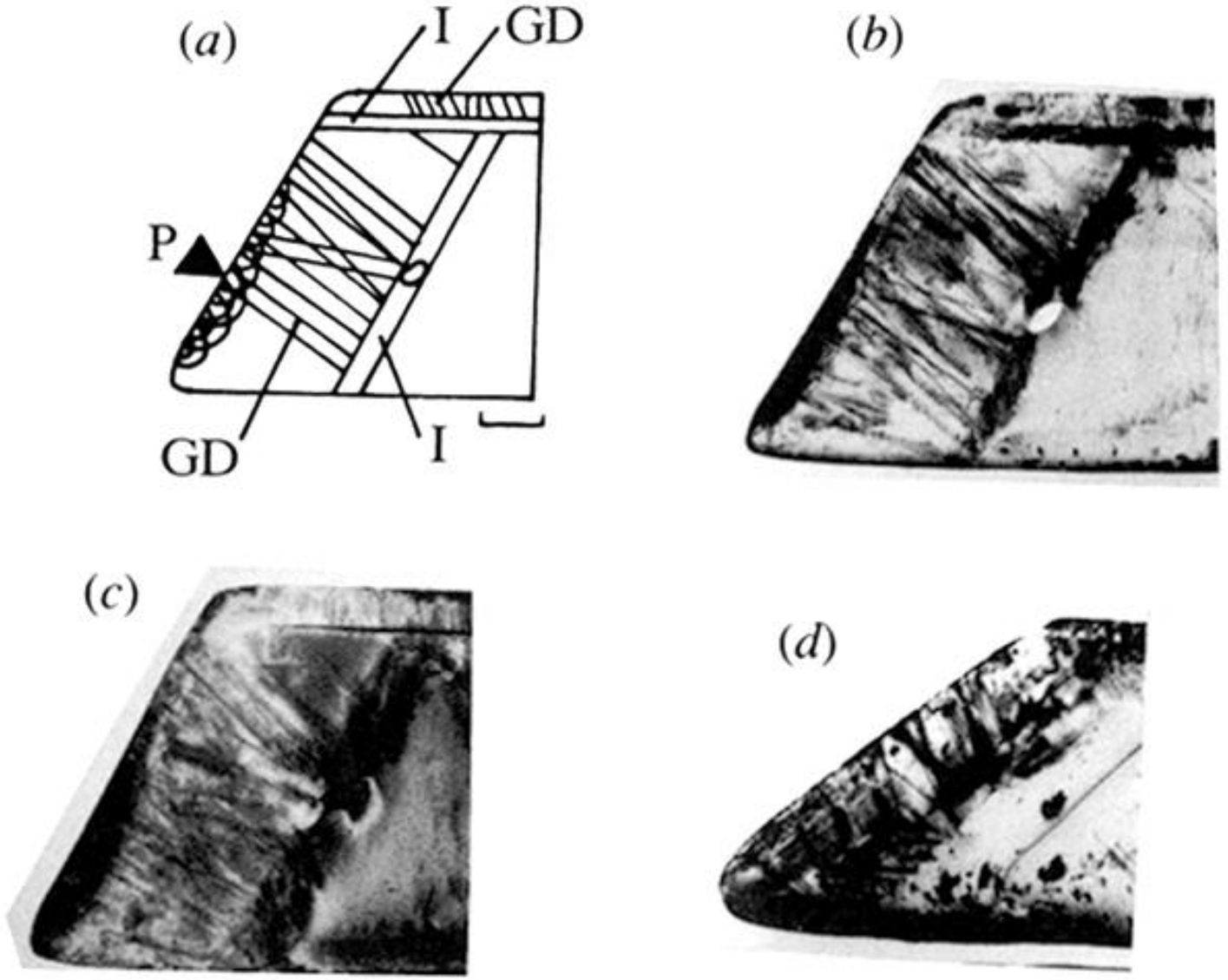

Figure 6. X-ray topographs of a (110) section of a PETN crystal which has been indented on a side (101) face. (*a*) Schematic diagram; (*b*) $2\bar{2}0$ reflection; (*c*) 002 reflection; (*d*) $21\bar{1}$ reflection. (P, point of indentation; GD, growth dislocations; I, solvent inclusions.) (Scale mark 1 mm.)